Volume 1 | Number 1 | Jan 2013 | Pages 1–100

Nanoscale

www.rsc.org/nanoscale

ROYAL SOCIETY OF CHEMISTRY

ROYAL SOCIETY OF CHEMISTRY

www.rsc.org/nanoscale

Nanoscale

Remarkable enhancement of the electrical conductivity of carbon nanostructured thin films after compression

Vasilios Georgakilas,*[a] Apostolos Koutsioukis,[a] Martin Petr,[b] Jiri Tucek[b] and Radek Zboril[b]

In this work, we demonstrate a significant improvement in the electrical conductivity of carbon nanostructured thin films, composed of graphene nanosheets and multiwalled carbon nanotubes, by compression/polishing. It is shown that the sheet resistance of compressed thin films of carbon nanostructures and hybrids is remarkably decreased in comparison with that of as-deposited films. The number of the interconnections, the distance between the nanostructures as well as their orientation are highly altered by the compression favoring the electrical conductivity of the compressed samples.

Electrical conductivity is considered as one of the most important and attractive properties of carbon nanoallotropes with graphenic structure.[1] Pristine graphene, carbon nanotubes, their hybrids and composites with polymers have been widely studied as conductive nanomaterials in a plethora of potential applications such as transparent conductive films in solar cells, displays, electrodes in batteries, supercapacitors, fuel cells, conductive inks for printable electronics, biosensors, etc.[2-7]

Recently, we presented a highly conductive hydrophilic hybrid comprising of pristine graphene nanosheets and hydroxy-functionalized multiwalled carbon nanotubes (MWNT-*f*-OH).[8] This highly water dispersible hybrid deposited on paper showed a sheet resistance (R_s) of 25 Ω/sq which is among the lowest values in the literature for these materials; when incorporated in polyvinyl alcohol (PVA) in a 20% w/w, a highly conductive polymer composite was assembled showing the lowest value of R_s = 1300 Ω/sq.[8]

In an effort to explore the electrical conductivity of carbon nanostructured hybrids and examining several different treatments, it was observed that R_s and, consequently, the electrical conductivity of thin films made up of carbon nanostructures or hybrids were improved by compressing the samples or polishing their surface. In this communication, we address a role of the compression and polishing of carbon

nanostructured thin films in the decrease in R_s and, hence, increase in the electrical conductivity. This phenomenon has been also reported by Megaridis et al.[9] in a recent article where polishing is highlighted as a technique that enhances the electrical conductivity of a composite of acrylic emulsions with multilayered graphene. Hu et al.[10] has also recently shown that compression improves the electrical conductivity of graphene laminates that were used as a low cost printed RF antenna. Except these studies, our work is the first systematic presentation of the efficiency of compression and polishing on the electrical conductivity of carbon nanostructured thin films in the literature.

In this study, we used pristine graphene nanosheets (*p*G) prepared by liquid exfoliation of graphite in DMF, pristine MWNTs, highly hydrophilic functionalized MWNTs (MWNT-*f*-OH) and the hybrid that was formed by combination of *p*G and MWNT-*f*-OH (*p*G/MWNT-*f*-OH). MWNT-*f*-OH and the hybrid were prepared following the procedures published elsewhere.[8,11]

The examined conductive thin films were round spots that were formed by the deposition on a sheet of paper of carbon nanomaterials from a liquid phase and air dried before the compression/polishing. In order to have comparable results, the deposited spots of several samples were formed by similar amounts of carbon nanostructures and the deposition, air drying, and compression were performed under exactly the same conditions with the exception of the solvent, since *p*G and pristine MWNTs were not dispersible in water or ethanol as the other two samples. The first step of the procedure involved the preparation of concentrated suspensions of carbon nanostructures. *p*G dispersion in dimethylformamide (DMF) with a final concentration of 1.4 μg/μl was formed by liquid exfoliation of graphite under sonication and consisted mainly of monolayer and few layered nanosheets (see details in the Experimental section).

Similarly, pristine MWNTs were also dispersed in DMF by sonication affording a suspension of 2 μg/μl. The sample of MWNT-*f*-OH was prepared as a concentrated suspension of 4 μg/μl in water since the strong hydrophilic nature of this

[a.] Department of Materials Science, University of Patras, 26504 Rio (Greece)
[b.] Regional Centre of Advanced Technologies and Materials, Department of Physical Chemistry, Faculty of Science, Palacky University in Olomouc, 17.listopadu 1192/12, 771 46 Olomouc (Czech Republic).

COMMUNICATION

product provides a high dispersibility in water.[11] The hybrid pG/MWNT-f-OH was prepared in a ratio of 14/1, following our previous work, to get a final suspension of 15 µg/µl in water.[8]

A certain amount of the samples was transferred on common paper by drop cast and air dried leaving circular black spots on the surface with a mean diameter of 5 mm. The paper acts as a filter and the solvent is mostly removed from the drop rather fast, leaving the carbon material homogeneously dispersed on the surface of the paper. This procedure is, in a small scale, similar to the vacuum filtration of graphene suspension that leads to the formation of graphene films.[12-14]

After a thorough air drying with low heating (40 ^{0}C), the samples were pressed by a common pressure machine. The R_s measurements were performed on the same samples before and after the exposure to the pressure to avoid the differences in the sample preparation.

The impact of the compression on R_s of all the samples by applying a pressure of 150 MPa for two minutes are presented in Table 1. Except pristine MWNTs, R_s of all the other samples decreased by 90% after the exposure of the samples to the pressure.

Table 1. The sheet resistance (R_s) of the carbon hybrid samples before (R_{s1}) and after compression (R_{s2}) or polishing** (* the sample was dried at 70 ^{0}C).

	Amount of carbon (µg)	R_{s1} (Ω/sq)	R_{s2} (Ω/sq)
pG	42	6000	550
Pristine MWNTs	60	3200	2400
MWNT-f-OH	40	4400	400
pG/MWNT-f-OH	300	140	14
pG/MWNT-f-OH *	300	600	14
pG/MWNT-f-OH **	300	140	35

The samples were exposed to even higher force and for longer time duration leading to the conclusion that the positive impact of the compression on R_s reaches a limit with the pressure of 150 MPa applied for two minutes. By increasing the pressure to, for example, 350 MPa or more, R_s often increased, indicating the formation of microcracks in the films.

In order to examine the effect of surface polishing instead of direct compression, the samples were softly polished by a glass rod with a smooth surface. After polishing, the samples similarly showed a decrease in R_s, however, at a moderate degree. A characteristic example is listed in Table 1; a thin film of the pG/MWNT-f-OH hybrid showed a decrease of 75% in R_s after polishing while in a similar sample after compression the decrease reached to 90%. Although the impact of polishing seems to be important, it was not possible to assess the direct effect of polishing since this technique always involves a low compression (estimated pressure 2,5 MPa, see also SI).

Fig. 1. Characteristic SEM images of (a-d) the hybrid pG/MWNT-f-OH and (e-h) the pG thin films before (left) and after compression (right).

The application of pressure on the samples has as a direct effect on a remarkable decrease of the surface roughness as depicted in SEM and AFM images of the products (see Fig. 1 and Fig. 3) and the compression of the as prepared - by the drop cast - films as revealed by the thickness of the samples before and after pressing using the SEM profile images (see Fig. 2). The changes in the appearance of the samples before and after pressure treatment are also seen in the transmission electron microscopy (TEM) images (see Fig. 4). MWNTs show a lower contrast in the pressed sample in comparison to that in the unpressed sample. The decrease in the MWNTs contrast implies suppression of the interface between MWNTs and graphene nanosheets and improved compactness of the hybrid, promoting thus an enhanced electrical conductivity of the hybrid after compression.
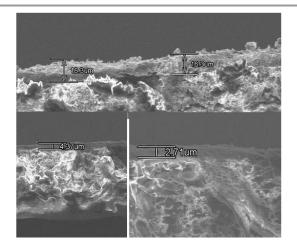
Fig. 2. Profile SEM images of *p*G/MWNT-*f*-OH before (upper) and after (down) the compression of the film. The mean thickness of the film of the *p*G/MWNT-*f*-OH hybrid was 17 μm before pressing and about 3.5 μm after pressing.
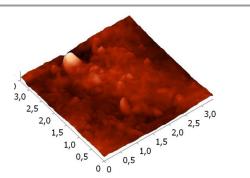

Fig. 3. A characteristic AFM image of the pressed *p*G/MWNT-*f*-OH hybrid (scale in nm).
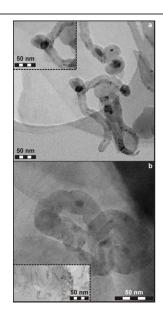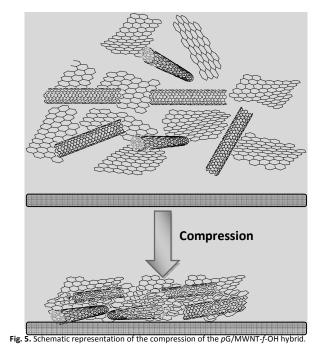

Fig. 4. Representative TEM image of (a) the unpressed *p*G/MWNT-*f*-OH hybrid and (b) the *p*G/MWNT-*f*-OH hybrid after pressure treatment.

The slow removal of the solvent mainly through the paper rather than evaporation after the drop cast restricts a dense stacking of the graphene nanosheets and MWNTs and favors the random settlement, leading to a low condensed thin film where carbon nanostructures are accommodated to have a limited number of extended interconnections. The random settlement of carbon nanostructures was further promoted if the removal of the solvent is accelerated by heating the sample during the procedure. As a consequence, the heated sample shows a much higher R_s (600 Ω/sq for the heated *p*G/MWNT-*f*-OH sample compared to 140 Ω/sq for the air dried sample) before pressing due to even lower density. The importance of compression was further confirmed by the fact that R_s of the heated sample after pressing reached R_s of the unheated sample (14 Ω/sq, see Table 1).
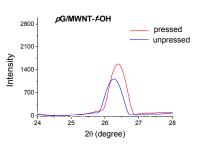

Fig. 5. Schematic representation of the compression of the *p*G/MWNT-*f*-OH hybrid.

Fig. 6. XRD diffraction pattern of the *p*G/MWNT-*f*-OH hybrid sample before and after compression.
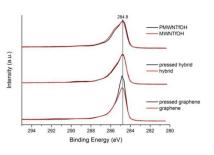
Fig. 7. X-ray photoelectron spectra of the pG, pG/MWNT-f-OH hybrid, and MWNT-f-OH thin films (red line) in comparison with their pressed samples (black line).

By applying a vertical external pressure on the sample surface, graphene nanosheets and carbon nanotubes are forced to compress and adopt a horizontal orientation not only in the surface but in the entire volume of the samples (Fig. 5). This compression-orientation is believed to result in a remarkable increase in the electrical conductivity of the films as indicated by the R_s measurements. By forcing carbon nanostructures to be organized in much less volume, the interconnections between the conductive parts are multiplied and probably become less resistive leading to a decrease in R_s which exceed 90% with pG, MWNT-f-OH, and pG/MWNT-f-OH hybrid and 25% in case of pristine MWNTs. The hybrid film (pG/MWNT-f-OH) with a final thickness of 2.7 μm after compression shows an electrical conductivity of 26000 S/m, which is among the highest values reported in the literature so far.[4,15-19]

Fig. 6 depicts the X-ray powder diffraction (XRD) patterns of pG/MWNT-f-OH hybrid samples before and after compression. The (002) peak at 26.2° for the unpressed hybrid indicates a mean interlayer spacing of 0.41 nm between the graphene nanosheets. After the compression, (002) peak is slightly shifted to 26.4° implying that the mean interlayer spacing decreased to 0.36 nm which is very close to the minimum spacing of the graphene packing at graphite (0.34 nm). The comparison of the X-ray photoelectron spectra (XPS) of graphene, MWNTs and the pG/MWNT-f-OH hybrid before and after compression is presented in Fig. 7. It shows the C1s spectra with the main peaks centered at 284.8 eV. As clearly seen, there is no significant chemical shift in the samples and the shapes of the compared spectra are identical. This unambiguously proves that there is no change in the chemical structure of the hybrid components during the compression.

Conclusions

In summary, the exposure of carbon nanostructured thin films to pressure and/or polishing resulted in a remarkable impact on their electrical conductivity as a consequence of the multiplication of the interconnections between the conductive nanostructures and the decrease of their electrical resistivity at the compressed films. Pressure and polishing are very simple techniques that could be applied to a great variety of devices made by printed or simply deposited carbon nanostructures.

Experimental

Preparation of graphene nanosheets dispersion. Pristine graphene nanosheets (pG) were isolated by the liquid exfoliation of 1 g graphite in 200 ml DMF under 5 h sonication in bath. The concentration of the afforded suspension after the removal of the unexfoliated graphite by centrifugation reached 0.35 μg/μl. The suspension was further ultracentrifugated (16000 rpm), the supernatant was removed and the precipitate redispersed in 50 ml of DMF leading to a final suspension of pG with a concentration of 1.4 μg/μl.

Measurements and characterization. Field emission scanning electron microscopy (SEM) images were taken on a Hitachi 6600 FEG microscope operating in the secondary electron mode and using an accelerating voltage of 5 kV. Transmission electron microscopy (TEM) images were taken on a JEOL JEM-2010 transmission electron microscope equipped with a LaB6 cathode operated at an accelerating voltage of 160 kV with a point-to-point resolution of 0.194 nm. A drop containing the sample dispersed in high-purity distilled water was placed onto a holey carbon film supported on a copper-mesh TEM grid (SPI Supplies, USA) and air-dried at room temperature. AFM images were obtained in tapping mode with a 3D Multimode Nanoscope, using Tap-300G silicon cantilevers with a tip radius <10 nm and a force constant of ≈20–75 N.m^{-1}. Sample of the pressed material was deposited onto silicon wafers (P/Bor, single side polished) from DMF suspensions by drop casting. X-ray photoelectron spectroscopy (XPS) measurements were performed under ultrahigh vacuum conditions with a base pressure of 1.4×10^{-7} Pa in a VersaProbe II (Physical Electronics, inc.) instrument equipped with a monochromatic AlK_α source (hv = 1486.7 eV) and a hemispherical analyser. Electrical measurements were performed using the four-probe technique, an AFX DC 9660SB power supply, and Keithley 2000 multimeter.

Acknowledgements

References

1   V. Georgakilas, J. A. Perman, J. Tucek and R. Zboril, *Chem. Rev.*, 2015, **115**, 4744.
2   E. B. Secor and M. C. Hersam, *J. Phys. Chem. Lett.*, 2015, **6**, 620.
3   X. Li, G. Zhang, X. Bai, X. Sun, X. Wang, E. Wang and H. Dai, *Nat. Nanotech.*, 2008, **3**, 538.
4   J. Wu, M. Agrawal, H.A. Becerril, Z. Bao, Z. Liu, Y. Chen and P. Peumans, *ACS Nano*, 2010, **4**, 48.
5   Y. Hernadez, V. Nicolosi, M. Lotya, F.M. Blighe, Z. Sun, S. De, I. T. McGovern, B. Holland, M. Byrne, Y. K. Gunko, J. J. Boland, P. Niraj, G. Duesberg, S. Krisnamurthy, R. Goodhue, J. Hutchison, V. Scardaci, A. C. Ferrari and J. N. Coleman, *Nat. Nanotechnol.*, 2008, **3**, 563.
6   C. Wu, X. Huang, G. Wang, L. Lv, G. Chen, G. Li and P. Jiang, *Adv. Funct. Mater.*, 2013, **23**, 506.

7   N. Behabtu, J. R. Lomeda, M. J. Green, A. L. Higginbotham, A. Sinitskii, D. V. Kosynkin, D. Tsentalovich, A. N. G. Parra-Vasquez, J. Schmidt, E. Kesselman, Y. Cohen, Y. Talmon, J. M. Tour and M. Pasquali, *Nat. Nanotech.*, 2010, **5**, 406.
8   V. Georgakilas, A. Demeslis, E. Ntararas, A. Kouloumpis, K. Dimos, D. Gournis, M. Kocman, M. Otyepka and R. Zboril, *Adv. Funct. Mater.*, 2015, **25**, 1481.
9   J. E. Mates, I. S. Bayer, M. Salerno, P. J. Carroll, Z. Jiang, L. Liu and C. M. Megaridis, *Carbon*, 2015, **87**, 3.
10   X. Huang, T. Leng, X. Zhang, J. C. Chen, K. H. Chang, A. K. Geim, K. S. Novoselov and Z. Hu, *Appl. Phys. Lett.*, 2015, **106**, 203105.
11   V. Georgakilas, A. Bourlinos, D. Gournis, T. Tsoufis, C. Trapalis, A. M. Alonso and M. Prato, *J. Am. Chem. Soc.*, 2008, **130**, 8733.
12   N. Behabtu, J. R. Lomeda, M. J. Green, A. L. Higginbotham, A. Sinitskii, D. V. Kosynkin, D. Tsentalovich, A. N. G. Parra-Vasquez, J. Schmidt, E. Kesselman, Y. Cohen, Y. Talmon, J. M. Tour and M. Pasquali, *Nat. Nanotech.*, 2010, **5**, 406.
13   L. Peng, Y. Feng, P. Lv, D. Lei, Y. Shen, Y. Li and W. Feng, *J. Phys. Chem. C*, 2012, **116**, 4970.
14   Z. Wu, Z. Chen, X. Du, J.M. Logan, J. Sippel, M. Nikolou, K. Kamaras, J. R. Reynolds, D. B. Tanner, A. F. Hebard and A. G. Rinzler, *Science*, 2004, **305**, 1273.
15   E.B. Secor, M.C. Hersam, *J. Phys. Chem. Lett*. 2015, **6**, 620–626.
16   L. Paliotta, G. De Bellis, A. Tamburrano, F. Marra, A. Rinaldi, S.K. Balijepalli, S. Kaciulis, M.S. Sarto, *Carbon* 2015, **89**, 260 – 271.
17   Z. Ji, J. Chen, L. Huang, G. Shi, *Chem. Commun.*, 2015, **51**, 2806-2809.
18   A.I.S. Neves, T.H. Bointon, L.V. Melo, S. Russo, I. de Schrijver, M.F. Craciun, H. Alves, *Scientific Reports* 2015, doi:10.1038/srep09866.
19   H. Sun, X. You, J. Deng, X. Chen, Z. Yang, J. Ren, H. Peng, *Adv. Mater*. 2014, 26, 2868–2873.